

Green Synthesis and Characterization of Biologically Synthesized and Antibiotic-Conjugated Silver Nanoparticles followed by Post-Synthesis Assessment for Antibacterial and Antioxidant Applications

Mehwish Mohy U Din, Andleeb Batool,* Raja Shahid Ashraf, Atif Yaqub, Aneeba Rashid, and Nazish Mohy U Din

Cite This: *ACS Omega* 2024, 9, 18909–18921

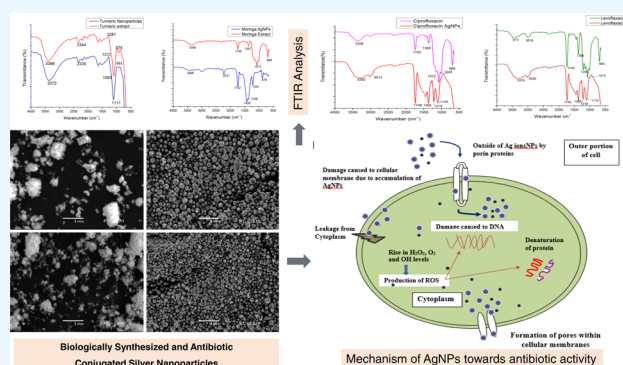
Read Online

ACCESS |

Metrics & More

Article Recommendations

ABSTRACT: The paper presents the antibacterial and antioxidant activities of silver nanoparticles (AgNPs) when conjugated with two antibiotics levofloxacin and ciprofloxacin as well as biologically synthesized nanoparticles from *Moringa oleifera* and *Curcuma longa*. Leaves of *Moringa* and powder of *Curcuma* were used in the green synthesis of silver nanoparticles. Ultraviolet–visible spectroscopy (UV), Fourier transform infrared spectroscopy (FTIR), and scanning electron microscopy (SEM) were used for the characterization of the synthesized silver nanoparticles. Comparison of levofloxacin and ciprofloxacin and their conjugated AgNPs was also studied for antibacterial and antioxidant activity. The synthesis of *Moringa*-AgNPs, turmeric-AgNPs, levofloxacin-AgNPs, and ciprofloxacin-AgNPs was confirmed by UV spectroscopy. An absorption peak value of 400–450 nm was observed, and light to dark brown color indicated the synthesis of AgNPs. *Moringa*-AgNPs revealed high antioxidant activity (80.3 ± 3.14) among all of the synthesized AgNPs. Lev-AgNPs displayed the highest zone of inhibition for *Staphylococcus aureus*, while in *Escherichia coli*, Cip-AgNPs showed high antibacterial activity. Furthermore, AgNPs synthesized using green methods exhibit high and efficient antimicrobial activities against two food-borne pathogens. Biologically synthesized nanoparticles exhibited antibacterial activity against *E. coli* (13.73 ± 0.46 with Tur-AgNPs and 13.53 ± 0.32 with Mor-AgNPs) and *S. aureus* (14.16 ± 0.24 with Tur-AgNPs and 13.36 ± 0.77 with Mor-AgNPs) by using a well diffusion method with significant shrinkage and damage of the bacterial cell wall, whereas antibiotic-conjugated nanoparticles showed high antibacterial activity compared to biologically synthesized nanoparticles with 14.4 ± 0.37 for Cip-AgNPs and 13.93 ± 0.2 for Lev-AgNPs for *E. coli* and 13.3 ± 0.43 for Cip-AgNPs and 14.33 ± 0.12 for Lev-AgNPs for *S. aureus*. The enhanced efficiency of conjugated silver nanoparticles is attributed to their increased surface area compared to larger particles. Conjugation of different functional groups contributes to improved reactivity, creating active sites for catalytic reactions. Additionally, the precise control over the size and shape of green-synthesized nanoparticles further augments their catalytic and antibiotic activities.



INTRODUCTION

Nanomaterials have gained extreme interest in the developing field of science and therapeutic medicines since the beginning of the 21st century.¹ The electronic, optical, catalytic, and magnetic properties of nanoparticles depend on their morphology, size, and chemical environments.² Among others, silver nanoparticles (AgNPs) have potential applications in various fields such as agriculture, waste management, forensic science, water treatment, pollution control, solar cells, and medicine.³ Till now, hazardous chemicals have been used as reducing agents in conventional methods for synthesizing AgNPs, which also require significant amounts of external heat energy. Hence, there is a need to synthesize AgNPs using

environment-friendly chemical processes to minimize the use of hazardous chemicals in the production of AgNPs.^{4,5} For the large-scale synthesis of metal and metallic oxide nanoparticles, plants are the best green source due to their diverse morphologies and sizes.⁶ The biomolecules, such as terpenoids, alkaloids, carbohydrates, and phenolic compounds,

Received: November 9, 2023

Revised: March 1, 2024

Accepted: March 27, 2024

Published: April 15, 2024



present in plant extracts are suitable for synthesizing silver nanoparticles. These nanoparticles can efficiently reduce metal ions into nanomaterials using a one-step procedure.⁷

The frequent utilization of antibiotics has led to the emergence of resistance among microorganisms. This resistance was initially characterized by microorganisms developing insensitivity to treatment, resulting in a decline in therapeutic effectiveness, heightened toxicity, the onset of side effects, nonspecific reactions, and difficulties in establishing appropriate dosing protocols.⁸ With the continuous increase in antibiotic resistance over the past decade, primarily driven by the widespread and inappropriate use of these medications, there has been a growing demand for more potent antibiotics.⁸ Nanoparticles (NPs) offer several advantages,^{7–10} including a high capacity for drug loading,⁸ an extended half-life, enhanced stability during transition,⁷ reduced toxicity, targeted delivery to specific sites, and the controlled release of therapeutic agents.¹⁰ When combined, these properties, along with the increased antibacterial activity stemming from high drug loading, improved drug availability, reduced toxicity, and prolonged the half-life of therapeutic agents, positioning nanoparticles as a promising approach to combat antibiotic resistance.⁹ Among various nanomaterials, metal nanoparticles (MNPs) stand out due to their pronounced antibacterial properties.¹⁰ The advanced drug delivery system of nanoparticles has developed several advantages such as increased solubility of the drug in blood serum, improved drug half-life in the body, and targeted release of drugs. These methods have been used in therapy with various drugs that target specific cells.¹¹ Drug-conjugated nanoparticles have been utilized to treat infections caused by microbial agents within cells. The process involves the entry of nanoparticles into host cells through endocytosis, followed by the release of drugs intracellularly.¹² This type of transport system works so fine that drug delivery systems of nanoparticles have now been accepted for medical trials and many nanoparticle formulations are under different stages of medical trials.¹³ In the treatment of microbial infections, antibiotic therapies have been found to be highly effective in the past few years, but bacterial strains have been resilient toward many drugs, causing great challenges to medical science. Multiple-drug resistance has reached an appalling situation. To decrease this problem, new initiatives and methods need to be established.¹⁴ One of these is the use of silver nanoparticles synthesized using plant parts.¹⁵

Hence, green chemistry application protocols are now gaining increasing reputation in environmental protection and wastewater treatment.^{16–19} Nanotechnology has an extensive range of applications in electronic, medical, commercial, and industrial fields.²⁰ Nanoparticles, such as silver, zinc oxide, platinum, gold, and palladium, are widely studied due to their unique characteristics when they are reduced in size from bulk materials to the nanoscale.²¹ The physicochemical properties of silver nanoparticles make them highly significant in the field of water treatment as well.²²

The synthesis of silver nanoparticles using biomolecules is gaining more importance due to its ecofriendly and green chemistry approach. The reducing power of biomolecules to convert Ag^+ to AgNPs is obtained from microorganisms and plants. The interface between microbes and metals helps researchers discover the synthesis of metallic nanomaterials, such as silver, platinum, and gold.²³ Silver metallic nanoparticles have been considered for their unique antimicrobial

properties. Silver nanoparticles not only affect the external surface of bacterial cells but also tend to penetrate the bacterial cell and hinder the functions of its intracellular proteins.²⁴

The trend of making and using nanoconjugates (a mixture of various kinds of nanoparticles) was not common previously. Therefore, no work has been reported simultaneously on biological and synthetic nanoconjugates of AgNPs. The novelty of this work is the synthesis and characterization of nanoconjugate AgNPs made from two plants, moringa and turmeric, and two antibiotics, levofloxacin and ciprofloxacin, and their comparative assessment for antibacterial and antioxidant applications has been done for the first time. The objective of this study is (i) to synthesize nanoparticles using biological sources and nanoconjugates with antibiotics to discover their antibacterial and antioxidant activity and (ii) to use nanoconjugates of antibiotics to enhance antibacterial efficacy, reduce resistance, improve bioavailability, enable targeted delivery, and minimize side effects in medical treatments. Characterization of stabilized biological nanoparticles, such as silver nanoparticles (AgNPs) and their nanoconjugates with antibiotics for bactericidal activity, is an important area of research in nanomedicine and antibacterial therapy.

■ MATERIALS AND METHODS

Chemicals. The chemicals and reagents used to synthesize moringa-AgNPs, turmeric-AgNPs, Cip-AgNPs, and Lev-AgNPs were silver nitrate (AgNO_3 , molecular weight (MW): 169.87 g mol^{-1} , 99% pure); trisodium citrate dihydrate ($\text{Na}_3\text{C}_6\text{H}_5\text{O}_7$, MW: 294.10 g mol^{-1} , 98% pure); sodium borohydride (NaBH_4 , molecular weight (MW) 37.83 g mol^{-1} , 97% pure); and sodium hydroxide (NaOH , molecular weight (MW) 39.997 g mol^{-1}) purchased from Sigma-Aldrich, Lahore, Pakistan. Levofloxacin (Lev, MW: 361.368 g mol^{-1}) and ciprofloxacin (Cip, MW: 367.9 g mol^{-1}) were purchased from Servaid Pharmacy, Lahore, Pakistan. All of the experimental processes were performed with deionized and double-distilled water. The media and reagents used for antibacterial applications were Muller–Hinton agar medium, nutrient broth, and 1,1-diphenyl-2-picryl-hydrazyl ($\text{C}_{18}\text{H}_{12}\text{N}_5\text{O}_6$) (DPPH, MW: 394.32 g mol^{-1}) from supplier Sigma-Aldrich, provided by GCU Lahore, Pakistan.

Biological Synthesis of Silver Nanoparticles. 10 g of turmeric powder (*Curcuma longa*) and drumstick tree (*Moringa oleifera*) was taken and mixed in 100 mL of deionized water. After that, the mixture was boiled and stirred on a hot-plate magnetic stirrer (CLV-CSL-DHOTRTIR, U.K.) for 10 min. The extract was filtered with Whatman cellulose filter papers (45 μm) and stored at room temperature until the completion of the experiment. 10 mL of aqueous solution of the extract was added to 60 mL of 1 mM silver nitrate solution dropwise throughout 30 s. A mixture of extract and silver nitrate was heated on a magnetic stirrer (C-MAG HS 4, IKA) at the temperature of 65 °C for almost 45 min until the color of the solution changed to dark-yellowish brown. This change in the color of the mixture showed the conversion of Ag^{\pm} ions to nanoparticles of silver (AgNPs).⁵ The stability of the nanoparticles was studied for 1 year.

Preparation of Nanoconjugates (NCGs). Selected antibiotics, i.e., levofloxacin and ciprofloxacin, were conjugated with optimized nanoparticles for evaluating their antibacterial efficacy. Levofloxacin-conjugated AgNPs (Levo-AgNPs) and ciprofloxacin-conjugated AgNPs (Cip-AgNPs) were synthe-

sized. Briefly, 5 mL (0.1 mM) of levofloxacin and ciprofloxacin solution was reacted with 5 mL (0.1 mM) of silver nitrate solution (AgNO_3) separately; the reaction mixture was magnetically stirred for 10 min. After that, 20 μL of 5 mM freshly prepared solution of sodium borohydride (NaBH_4) was added to the reaction mixtures. The yellow-brown color of the solution appeared due to the addition of a reducing agent, which indicated the silver ion reduction and formation of Lev-AgNPs and Cip-AgNPs. Freshly synthesized AgNPs were centrifuged (M-80, Beijing, China) at 12,000 rpm for 1 h after the supernatant was collected, and an antibiotic was prepared.²⁵ The stability of conjugated particles was checked for 1 year.

Characterization of Nanomaterials. The synthesized products were characterized using several procedures. Physiological characteristics like stability, size, and shape of conjugated AgNPs were determined by retaining different characterization methods, i.e., UV–visible spectroscopy (AE-S70-1U), Fourier transform infrared spectroscopy (FTIR) (Shimadzu IR Prestige21, Japan), and scanning electron microscopy (SEM)-JEOL (JSM-6480LV, Japan) in the CASP Department, Government College University, Lahore, Pakistan, with 15 kV acceleration. The reduction of Ag^{\pm} ions to AgNP ions was confirmed by measuring the spectrum of AgNPs after dilution using a Jasco V-630 spectrophotometer (JASCO Corporation, Japan) in the Zoology department of GCU, Lahore, Pakistan, operated within the range of 300–600 nm. UV was used for some time to check the stability of nanoparticles.

Maintenance and Confirmation of Bacterial Strains. In the current study, we use *Staphylococcus aureus* and *Escherichia coli* strains collected from clinical specimens from the laboratory of Ganga Ram Hospital, Lahore (31.5556° N, 74.3219° E). Bacterial strains were identified based on the biochemical tests, including Gram staining, growth in cetrimide agar, MacConkey agar, citrate utilization, and oxidase test. Strains of bacteria were grown at 37 °C for 15–18 h in nutrient broth medium. Overnight cultures were inoculated into fresh medium. For the determination of antibiotic activity, cells in the mid-exponential phase (optical density at 600 nm of 0.5–0.6) were used.

Antibacterial Activity. The antibacterial activity of the synthesized AgNPs, extracts, and antibiotics was determined against *E. coli* and *S. aureus*. Bacterial pure cultures were subcultured on agar-solidified (LB) medium. 25 μL of bacteria (1.0×10^6 colony-forming units (CFU)/mL) was swabbed onto the solidified agar plates using a swab. Then, the synthesized AgNPs and antibiotics were loaded into wells in three different quantities, i.e., 25, 50, and 100 $\mu\text{g}/\text{mL}$, for the antibacterial assay, while deionized water was used as a control. Plates were incubated at 37 °C overnight in the incubator. The zones of inhibition around the wells were measured by using a conventional ruler.

Antioxidant Activity. The AgNPs of *Moringa* extract, turmeric extract, ciprofloxacin, and levofloxacin were investigated for antioxidant activity using the previously used scavenging method of 2,2-diphenyl-1-picrylhydrazyl (DPPH) free radicals^{26,27} with methanol used as the negative control, while ascorbic acid was used as the positive control.²⁸ DPPH radical scavenging is a fast and easy decolorant process. A deep-violet color solution of 1,1-diphenyl-2-picrylhydrazyl is used in the oxidized form with an antioxidant compound, which results in DPPH reduction when the color appears

yellow from the deep-violet color. For the reaction, 2 mL of DPPH standard solution of 0.1 mM was added to 1 mL of freshly prepared sample solution of AgNPs to obtain various concentrations of 25–100 $\mu\text{g}/\text{mL}$. Standard ascorbic acid diluted solution (2 mL of DPPH and 1 mL of methanol) was also run with the samples. The mixture was properly shaken and stored in the dark at room temperature for an incubation of 1 h. The results of DPPH radical scavenging activity were found by measuring the absorbance (Abs) of every solution using a UV–visible spectrophotometer at 517 nm and estimating the percentage inhibition (I%) by using eq 1²⁴

$$\begin{aligned} \text{I\% inhibition of DPPH} \\ = \frac{(\text{Abs control sample} - \text{Abs test sample})}{\text{Abs control sample}} \times 100 \end{aligned} \quad (1)$$

By finding the half-maximal inhibitory concentration (IC_{50}) of each sample, antioxidant capacity was also evaluated, which was the concentration of the test sample that could inhibit 50% of the DPPH radicals and was computed in parallel from the linear plot of the ascorbic acid standard.

Data Analysis. All calculations and statistical analyses were performed on SPSS v22.0. SEM images were analyzed using ImageJ software. All graphical presentations were prepared in Origin and Microsoft Excel 2013.

RESULTS AND DISCUSSION

Biosynthesis of AgNPs. The biosynthesis of AgNPs was accompanied by a distinct color change. The color change indicated the synthesis of AgNPs as shown in Figure 1. The

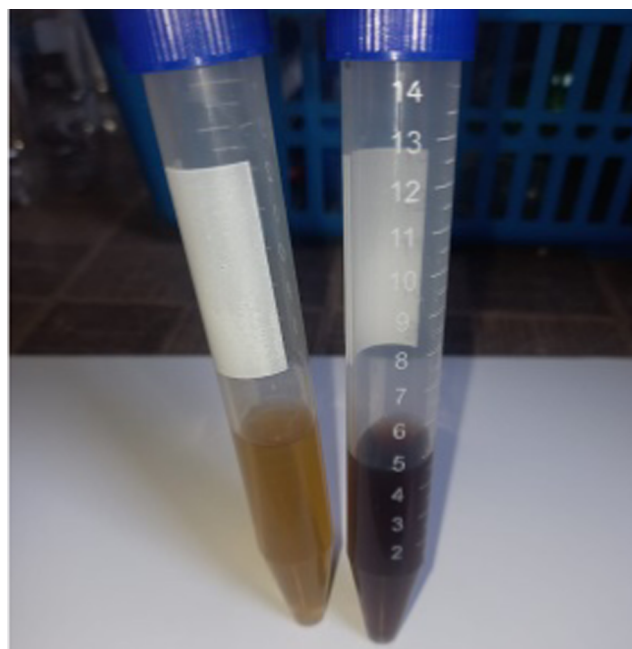


Figure 1. Change in color from yellowish (before) to dark reddish brown (after).

phenomenon of surface excitation of silver metal plasmon resonance results in the color change of the aqueous solution.²⁹ High levels of terpenoids and some proteins are present in the turmeric powder. Furthermore, turmeric is very rich in chemicals such as phellandrene, zingiberene, sabinene, and sesquiterpenes. Many of these described compounds are

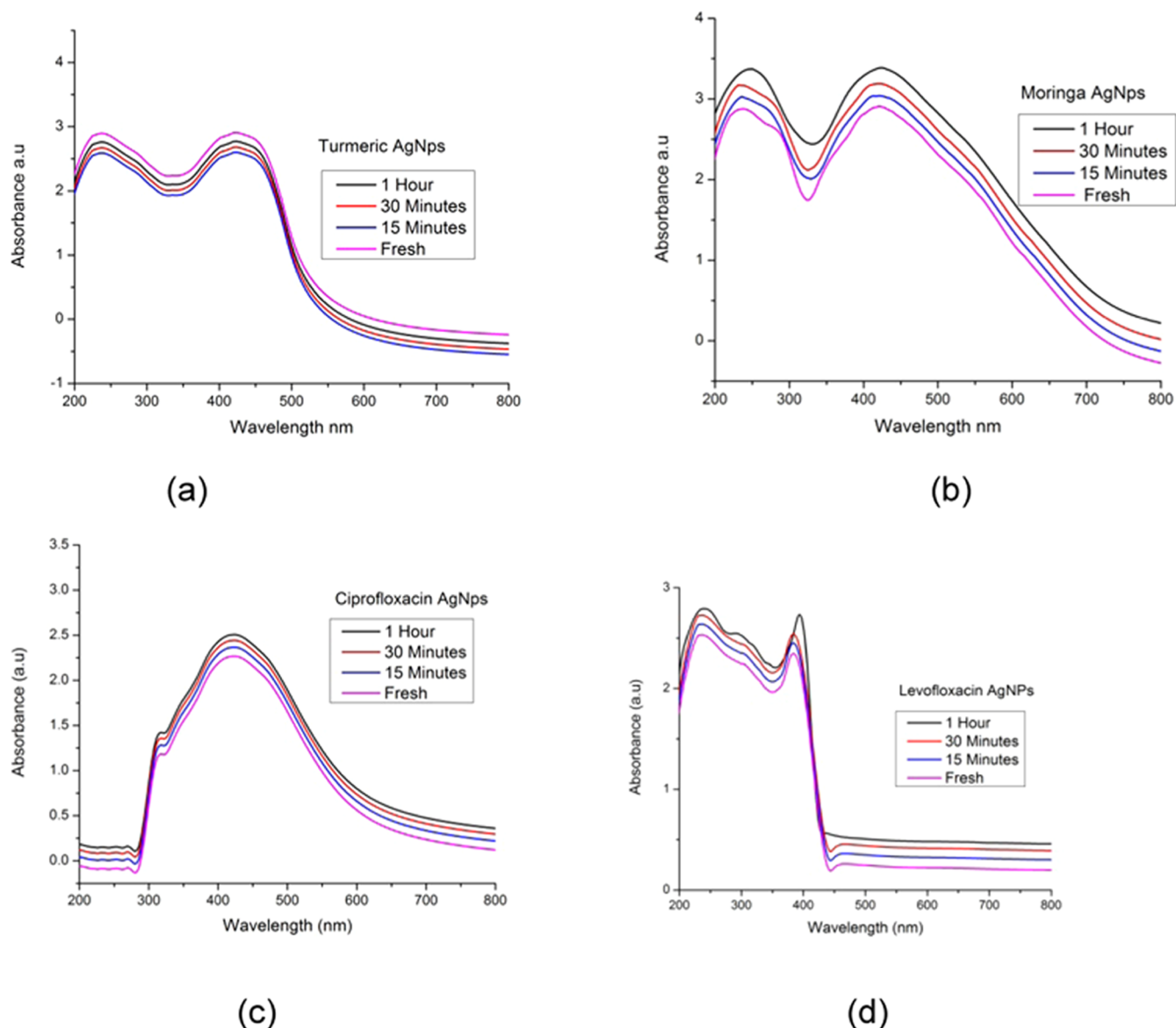


Figure 2. UV spectra of silver nanoparticles: (a) Tur-AgNPs, (b) Mor-AgNPs, (c) Cip-AgNPs, and (d) Lev-AgNPs at different time intervals.

polyphenolic biologically active elements known as curcumin, which results in their unique color and flavor.³⁰

The first indicator of silver nanoparticles is the color change from light yellowish to dark reddish-brown color as shown in Figure 1. The maximum absorbance of the turmeric leaf extract was measured at 433 nm, while that of the *Moringa* leaf extract was 445 nm; Cip- and Lev-conjugated AgNPs showed a peak at 420 and 412 nm, respectively. Color change in the biologically synthesized nanoparticle solution was due to the occurrence of surface plasmon resonance in metal nanoparticles³¹ as a result of the reduction of silver ions into nanoparticles of silver.

Time-dependent kinetic study for the synthesis of AgNPs from *turmeric*, *Moringa*, ciprofloxacin, and levofloxacin was carried out at different time intervals after the addition of Ag⁺ ions into the flask. Figure 2a–d shows the evolution of silver nanoparticle synthesis with time. Synthesis of silver nanoparticles was seen within 1 h after the addition of salt in culture medium at room temperature. The production of nanoparticles showed exponential growth up to 1 h of the current study. A

vast absorption peak appeared at $\lambda_{\text{max}} = 430$ nm and significant absorption exists at >700 nm with time lapse, which represents the characteristic SPR of aggregated and spherical AgNPs.

Tur-AgNPs were found to be stable 1 year after synthesis with a red shift in peak absorbance (Figure 2). The long-term stability and effectiveness of turmeric nanoparticles, spanning a year or more, may vary due to factors such as the manufacturing process, storage conditions, and potential interactions with their environment. Researchers have documented that proteins present in turmeric powder contribute to the stabilization of biosynthesized silver nanoparticles (AgNPs). The stabilization is facilitated through cysteine or free amino group residues present in the proteins, acting as capping agents for AgNPs. These capping agents play a crucial role in safeguarding the nanoparticles from aggregation, thereby maintaining their stability.³² To maintain their activity, it is essential to store turmeric nanoparticles correctly and continuously assess their stability using suitable testing and analysis methods. Conjugated nanoparticles may face challenges in terms of stability over time. Aggregation or

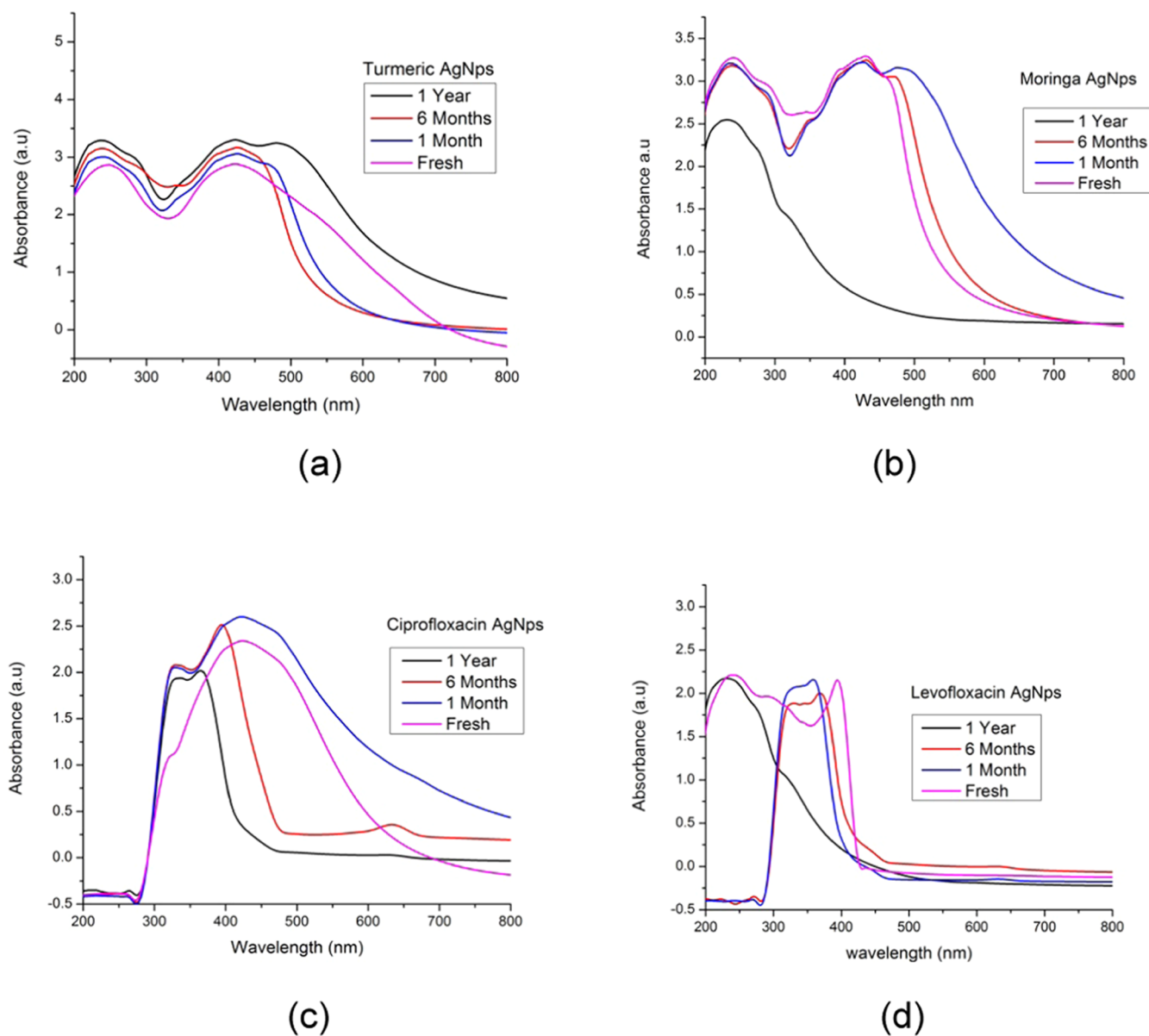


Figure 3. UV–visible spectroscopy of silver-conjugated nanoparticles at different times of the year: (a) turmeric AgNPs, (b) *Moringa*-AgNPs, (c) ciprofloxacin-AgNPs, and (d) levofloxacin-AgNPs.

degradation of nanoparticles can impact their efficacy, especially in applications where stability is crucial,³³ while in *Mor*-AgNPs, a slight change in peak absorbance occurred with a blue shift in the peak over time. The peak of the particles finally disappeared after 1 year (see Figure 3b). A red shift in the peaks of nanoparticles, along with a slight reduction in absorbance, was also observed for ciprofloxacin and levofloxacin-AgNPs (Figure 3c,d). However, a reduction in absorbance was observed over time. The reason for the difference in time may be due to the fact that silver nanoparticles are prone to instability over time due to several factors: aggregation, oxidation, surface modification contaminants, and size changes.²¹ (Figure 3d).

Scanning Electron Microscopy and Size Distribution of Silver Nanoparticles. This method allowed for obtaining both quantitative and qualitative data as well as other details related to nanoparticle size and morphology.³² Scanning electron microscopy revealed the synthesis of uniformly

spherical-shaped Lev-AgNPs (see Figure 4d) with a 100 nm average size range and 12% polydispersion. Cipro-AgNPs displayed an average size of 100 nm with polydispersity in Figure 4c.³² The shapes of *turmeric* and *Moringa*-AgNPs particles showed agglomeration and aggregation (see Figure 4a,b). *Turmeric* AgNPs display an average size of 70 nm with irregular surface morphology and polydispersity, while *Moringa* nanoparticles were created with an average size of 80 nm; some of the spherical particles were seen prominently in good concentration (see Figure 5). *Tur*-AgNPs exhibited a spherical-shaped morphology with a composite level of particle clusters. These NPs showed 7% polydispersity (Figure 4a).

FTIR of Silver-Conjugated Nanomaterials. The FTIR peaks of silver nanoparticles appeared at 1111, 1093, 1272, 2335, and 3373 cm^{-1} . At 600–1400 cm^{-1} , the peaks appear to be due to C–N and C–O carboxyl groups due to extensions of amide bonds present in proteins;²⁹ these are due to a high content of proteins present in plant leaves. The peak at 1550

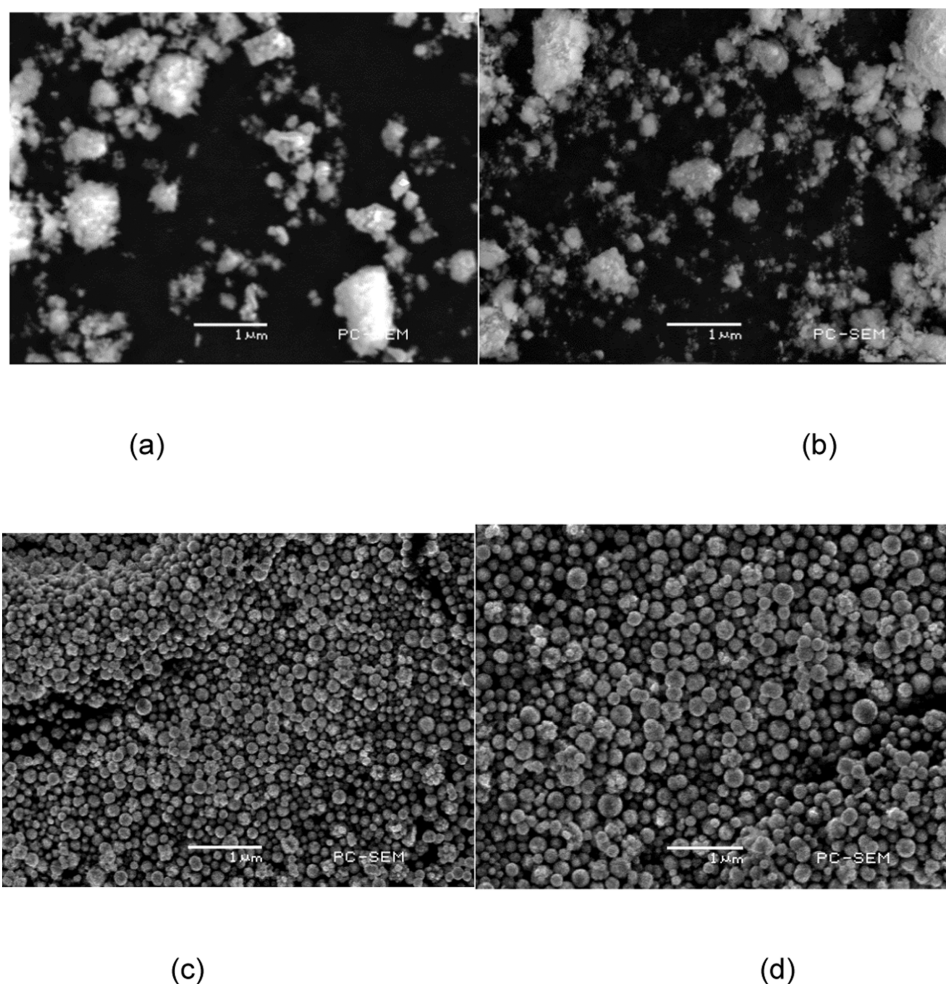


Figure 4. SEM images of the AgNPs: (a) Tur-AgNPs, (b) Mor-AgNPs, (c) Cip-AgNPs, and (d) Lev-AgNPs.

cm^{-1} is due to the nitrile group that contains the $\text{C}\equiv\text{N}$ group, which indicates a triple bond between nitrogen and carbon, whereas the peak at 1690 cm^{-1} refers to the $\text{C}=\text{O}$ and $-\text{C}\equiv\text{C}-$ bond, which is primary and secondary fission; peaks at 2335 cm^{-1} refer to the CN function, while the peak at 3373 cm^{-1} specifies the existence of the $\text{O}-\text{H}$ bond of phenolic compounds. Phenolic groups and proteins work as reducing and stabilizing factors and after linking with AgNPs may result in clustering through free amino groups or the residue of cysteine.³²

The functional groups of ciprofloxacin were identified using FTIR spectroscopy in the scan range of $4000-500\text{ cm}^{-1}$. The FTIR spectrum obtained for ciprofloxacin (Figure 6c) exhibits many absorption peaks like 3359 cm^{-1} assigned for the $\text{O}-\text{H}$ bond of alcohols/phenols, 3031 cm^{-1} for the $\text{N}-\text{H}$ bond of ammonium ions, 1740 cm^{-1} for the $\text{C}=\text{O}$ bond of carboxylic acids, 1365 cm^{-1} for the $\text{N}-\text{H}$ bond of ammonium ions, 1219 cm^{-1} for the $\text{N}-\text{O}$ bond, 1073 cm^{-1} for $\text{C}-\text{O}$ of ether bond, 1005 cm^{-1} for the $\text{C}-\text{N}$ bond of amines, 750 cm^{-1} for the $\text{C}-\text{H}$ bond of aromatic benzene, and 689 cm^{-1} for the $\text{O}-\text{H}$ bond of alcohols/phenols,³⁴ whereas FTIR spectra of ciprofloxacin-conjugated AgNPs (Figure 6b) showed 3282 cm^{-1} assigned for the $\text{O}-\text{H}$ bond of alcohols/phenols and 1748 cm^{-1} for the $\text{O}-\text{H}$ bond of primary amines. Based on FTIR analysis, it is confirmed that the broad peaks of phenols (3325 cm^{-1}) and primary amines of proteins (1636 cm^{-1}) are interacting with biosynthesized SNPs and acting as reducing agents (Figure

6c). The interaction between the $\text{C}=\text{O}$ of the functionalized CIP and AgNPs through a hydrogen (H) bond indicated their successful attachment.³⁵ The transmittance peak at 1272 cm^{-1} was due to the amine ($\text{C}-\text{N}$) piperazine group of the CIP. In addition, the aryl $\text{C}-\text{H}$ and $\text{C}-\text{N}$ stretching peaks were found at 2919 and 1094 cm^{-1} , respectively, in agreement with the previous observations.³⁶

The FTIR analysis of the *Moringa* extract and *Moringa*-AgNPs confirmed the existence of common absorption bands (Figure 6b). These bands relate to functional groups that might be involved in silver ion reduction as well as stabilization of synthesized AgNPs. Broad intense bands observed at 3466 , 3359 , and 3003 cm^{-1} (Figure 6b) are characteristics of all polysaccharides due to the $-\text{OH}$ stretch.³⁷ The polar groups, $-\text{OH}$, are strongly capable of coordinating bonds with metal ions (e.g., with silver ions).³⁸ The bands at 1732 and 1646 cm^{-1} relate to the $-\text{C}=\text{O}$ stretch and the bands around $\sim 1400\text{ cm}^{-1}$ confirm the presence of the carboxylic acid in uronic acids, which is associated with metal chelation and result in the reduction of toxicity of metal.³⁹ As recommended by the FTIR data, polysaccharides are bound to the surface of nanoparticles through hydroxyl and carboxyl groups. The *Moringa* leaf extract consists of protein, phenols, terpenoids, and carboxylic acid, which result in the synthesis and reduction of nanoparticles.⁴⁰

However, in Figure 6d for AgNPs for levofloxacin, peaks were found at 3310 and 3030 cm^{-1} , which indicate the

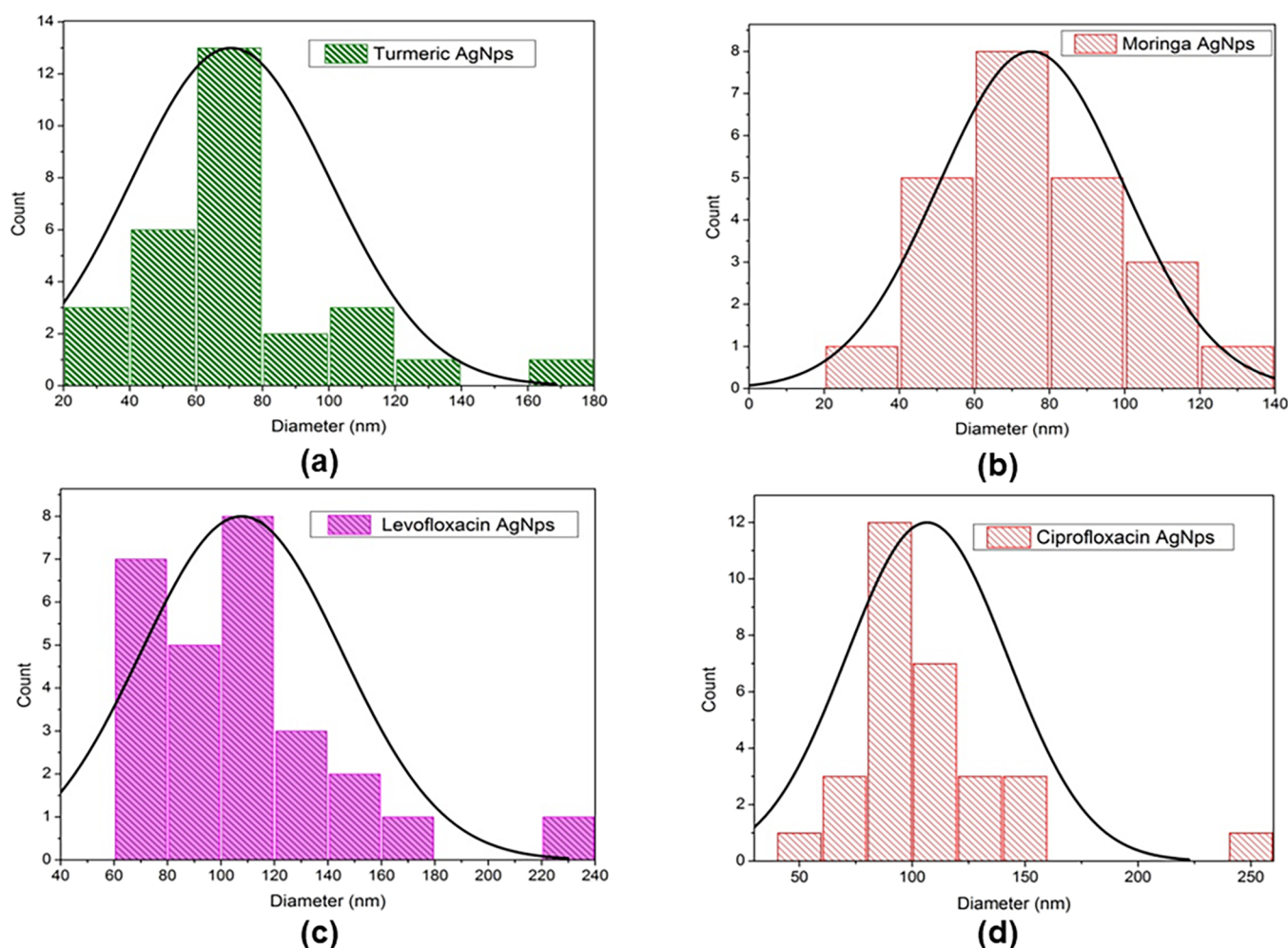


Figure 5. Size distribution maps of (a) Tur-AgNPs, (b) Mor-AgNPs, (c) Lev-AgNPs, and (d) Cip-AgNPs.

presence of amide bonds, while small peaks were found between 2000 and 3000 cm^{-1} , which show the presence of carboxylic acid and C–N bonds. A peak at 1740 cm^{-1} observed in levofloxacin and Lev-AgNPs is due to ketones present in the solution. Peaks at 1219 and 1110 cm^{-1} indicate alkyl ketones and alkyl amines present in Lev-AgNPs.⁴¹

Antibacterial Activity. In this study, both Gram-negative (*E. coli*) and Gram-positive (*S. aureus*) food-borne pathogenic bacteria were employed to assess the antibacterial activity of AgNPs. The antibacterial activity of silver nanoparticles conjugated with turmeric showed a larger zone of inhibition at a concentration of 100 $\mu\text{g}/\text{mL}$. The inhibition zone measured 13.53 mm in *E. coli* (Figure 7). Moringa-conjugated silver nanoparticles display a zone of inhibition of 13.73 mm at a concentration of 100 $\mu\text{g}/\text{mL}$. The zone of inhibition for antibiotic-conjugated silver nanoparticles tends to be higher than that of biologically synthesized nanoparticles, measuring 14.4 and 13.93 mm for Cip-AgNPs and Lev-AgNPs, respectively, at a concentration of 100 $\mu\text{g}/\text{mL}$. As shown in Figure 7, after being conjugated with AgNO_3 , ciprofloxacin and levofloxacin exhibit a larger zone of inhibition compared to their original forms. In their pure form, these antibiotics exhibit a zone of inhibition measuring 13.3 and 14.33 mm at a concentration of 100 $\mu\text{g}/\text{mL}$, respectively.⁴² Chemically synthesized AgNPs exhibit a zone of inhibition measuring 7.3 mm at a concentration of 100 $\mu\text{g}/\text{mL}$. In the current study,

no zone of inhibition was observed with the extracts of turmeric (T-E) and Moringa (M-E). Tur-AgNPs exhibited remarkable efficacy in the degradation of the primary contaminant found in drinking water and wastewater, namely, *E. coli*. When treated with Tur-AgNPs, a substantial reduction was observed in the CFU/mL *E. coli*.⁴³ To evaluate its effectiveness, contaminated water must be treated with Tur-AgNPs.

In the present study, the antibacterial activity of Mor-AgNPs was observed (Figure 8) with a zone of 13.36 mm and Tur-AgNPs showed a zone of 14.16 mm with 100 $\mu\text{g}/\text{mL}$ in *S. aureus*. Moringa is generally considered safe and has been used traditionally for various health purposes. The conjugation with silver nanoparticles can potentially improve the biocompatibility, making it suitable for biomedical applications. Moringa conjugated with silver nanoparticles offers several advantages for antibacterial and antioxidant applications, but challenges related to standardization, biocompatibility, regulatory approval, quantitative control, and interaction complexity should be carefully addressed for successful and safe implementation. Cip-AgNPs and Lev-AgNPs showed 11.66 + 0.32 and 7.3 mm zones of inhibition, respectively. As shown in Figure 8, the bactericidal property of these biologically synthesized AgNPs is due to the release of cations of silver; these Ag^{\pm} ions get attached to the cell wall of bacteria due to electrostatic attraction, and these ions also penetrate inside the bacteria.

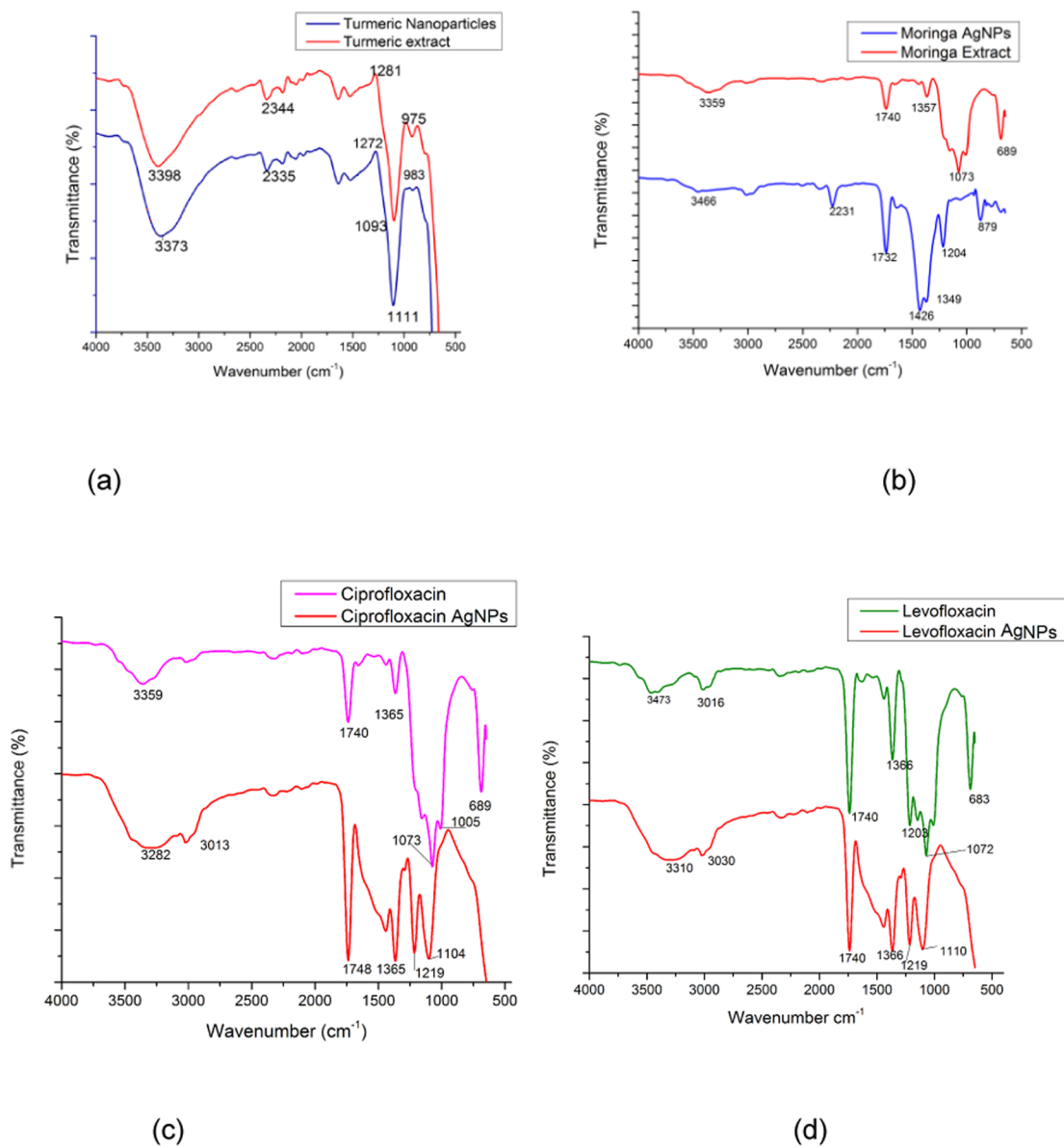


Figure 6. Fourier transform infrared spectrum of silver-conjugated nanoparticles: (a) turmeric AgNPs, (b) *Moringa*-AgNPs, (c) ciprofloxacin-AgNPs, and (d) levofloxacin-AgNPs.

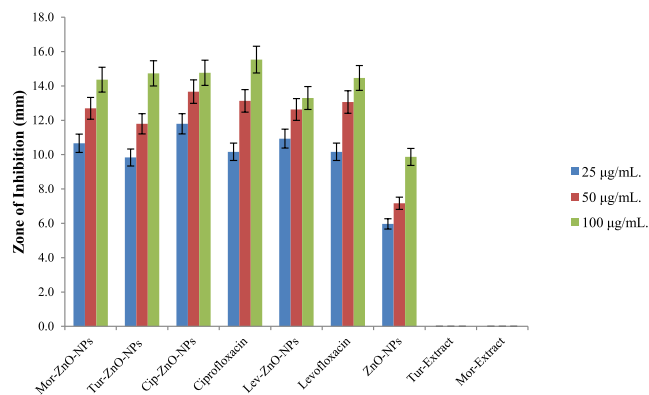


Figure 7. Zone of inhibition of *E. coli* for AgNPs for 24 h. T-E (turmeric extract) and M-E (*Moringa* extract) did not show any antibacterial activity.

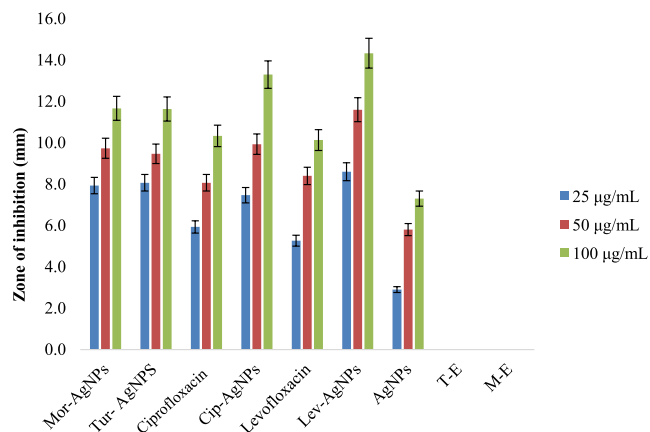


Figure 8. Zone of Inhibition of *S. aureus* AgNPs for 24 h. Silver nanoparticles conjugate T-E (turmeric extract) and M-E (*Moringa* extract) did not show any antibacterial activity.

The antibacterial activity of Lev-AgNPs was higher than that of free levofloxacin against *S. aureus*.⁴⁴ Stable Mor-AgNPs produced with a biological method by using *Moringa* leaves have good antibacterial activity against both Gram-negative and Gram-positive bacteria usually found in wastewater.⁴⁵ Indeed, Mor-AgNPs demonstrate notable efficiency as catalysts for the degradation of organic dyes under sunlight exposure. This degradation process occurs precisely on the surface of AgNPs, where they serve as catalysts.⁴⁶ Mor-AgNPs have demonstrated remarkable effectiveness in the removal of lead (Pb) from contaminated water.⁴⁷ Recent findings suggested that Mor-AgNPs show substantial potential for utilization in water treatment due to their ability to operate without generating toxic or hazardous chemicals throughout the treatment process. In broad terms, the bactericidal effect of silver nanoparticles (AgNPs) is ascribed to their interaction with the bacterial cell wall. This interaction results in the accumulation of envelope protein precursors, leading to protein denaturation, a decrease in proton motive force, and ultimately cell death. This mechanism underscores the antimicrobial properties of AgNPs and is a key factor in their exploration for various applications, ranging from medical contexts to water treatment and beyond.⁴⁸

Silver has been reported many times as a strong agent with higher antibiotic resistance in bacteria due to its multitargeted action.⁴⁹ Silver nanoparticles' mode of action is to destroy the bacterial cell wall, resulting in a change in the structure of the cell wall. As a result, the bacteria become more susceptible to antibiotics.⁵⁰ Silver nanoparticles possess unique thermal and electrical properties as well as a high surface area-to-volume ratio. This characteristic allows them to interact with the surface of bacteria, resulting in antimicrobial activity. Due to differences in the cell membrane structure, there is a variation in antibacterial activity. The Gram-negative bacteria have a phospholipid layer, while Gram-positive bacteria have a peptidoglycan outer layer. Therefore, both types of bacteria undergo different mechanisms in the presence of turmeric,⁵¹ while previous study reveals that curcumin is similarly effective against both Gram-negative and Gram-positive bacteria.⁵² Turmeric, specifically its active compound curcumin, is known for its strong antibacterial properties. When conjugated with silver nanoparticles, it can enhance and broaden the antibacterial spectrum, making it effective against a variety of bacterial strains.⁵³ Moreover, the present study found that turmeric AgNPs exhibit higher antimicrobial activity compared to curcumin against both pathogens.⁵⁴ Free radicals produced by silver nanoparticles inhibit bacterial growth. Silver cations are released when nanoparticles dissolve in water or penetrate cells.⁵⁵ These silver ions attach to the cell membrane, nucleic acids, and proteins. They cause deformations and structural changes in bacterial cells and are also involved in the production of reactive oxygen species. This disables many enzymes by targeting their thiol groups. DNA modification also occurs as a result of silver ions, which lead to the death of bacterial cells.⁵⁶ The use of turmeric in the synthesis process aligns with green chemistry principles, making the process environmentally friendly compared to traditional chemical methods.

The overall mechanism of conjugated AgNPs is also analyzed and provided in the figure below (Figure 9).

Biologically synthesized silver nanoparticles exhibited antimicrobial activity against pathogenic microorganisms, as made evident by the diameter of the zone of inhibition. The

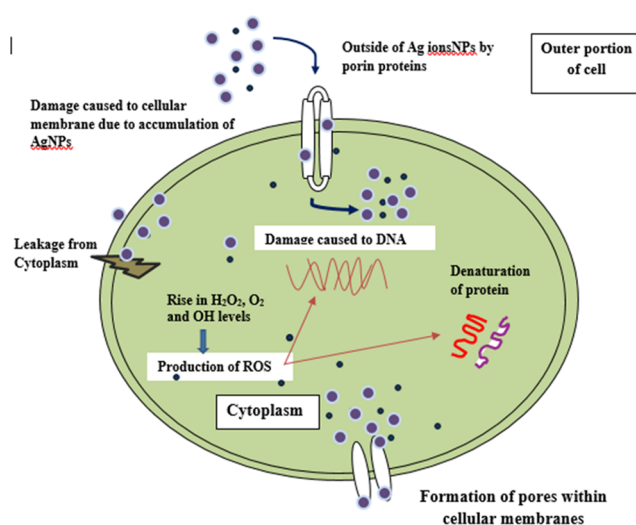


Figure 9. Mechanism of conjugated AgNPs toward antibiotic activity.

Gram-negative bacteria *E. coli* showed a larger inhibition zone compared to the Gram-positive bacteria *S. aureus* due to variations in the composition of their cell walls.⁵⁷ Gram-positive bacteria contain a thick peptidoglycan cell wall consisting of cross-linked short peptides with linear polysaccharide chains. This structure establishes a more solid assembly, which may hinder the penetration of silver nanoparticles. In contrast, Gram-negative bacteria have a thinner peptidoglycan layer in their cell wall. Several main mechanisms contribute to the biocidal properties of silver nanoparticles against various microorganisms. First, the silver nanoparticles disrupt the cell wall and cell membranes of microorganisms by attaching to the negatively charged cell surface. This damages their important functions, such as electron transport, permeability, respiration, and osmoregulation.⁵⁸ Second, silver nanoparticles damage the cell wall of bacteria by penetrating the cell and interacting with proteins, DNA, and other sulfur- and phosphorus-containing cell components. Third, the silver nanoparticles in the microorganism release silver ions, which have a biocidal effect that depends on their size and dosage.^{59,60} The combination of silver nanoparticles and the antibiotic levofloxacin showed a synergistic effect due to increased antibacterial activity, lowered antibiotic dosage, reduced resistance development, and broadened spectrum, enhancing the antimicrobial activity against *S. aureus* and *E. coli*.⁶¹

Antioxidant Activity. The DPPH radical was used to determine the antioxidant activity of naturally occurring compounds because it is stable as a free radical.⁶² Plant extracts contain polyphenolic components that exhibit antioxidant activity. This is because they can donate electrons and hydrogen atoms while capturing free radicals. As a result of this reaction, the purple color 2, 2-diphenyl-1-picrylhydrazyl (DPPH) is reduced to α , α -diphenyl- β -picrylhydrazine, resulting in a change to a yellow color.^{63,64} The results of the free radical scavenging activity of plant extracts are listed in Table 1. Results showed that Mor-AgNPs exhibited the highest DPPH radical scavenging activity ($80.3 \pm 3.14\%$) at a concentration of $100 \mu\text{g/mL}$, followed by Tur-AgNPs with an activity of $75.22 \pm 2.8\%$ at the concentration of $100 \mu\text{g/mL}$. Turmeric is a well-known antioxidant, and curcumin, its major component, has strong antioxidant effects. Conjugating with silver nanoparticles may amplify these antioxidant properties,

Table 1. In Vitro Antioxidant Activity of AgNPs; DPPH Scavenging Activity of Different Conjugates Compared to the Ascorbic acid as a Standard Antioxidant, the data have been shown with mean \pm SD value with $n = 3^a$

Samples	Concentration of DPPH ($\mu\text{g mL}^{-1}$)	ScaSvenging (%)	IC ₅₀ ($\mu\text{g mL}^{-1} \pm \text{SEM}$)
<i>Moringa</i> AgNPs	25	20.57 \pm 2.19	2.54 \pm 0.08
	50	44.91 \pm 10.59	
	75	57.46 \pm 4.15	
	100	80.3 \pm 3.14	
Turtrmeric AgNPs	25	11.05 \pm 4.4	8.87 \pm 0.07
	50	26.97 \pm 5.55	
	75	47.65 \pm 4.5	
	100	75.22 \pm 2.8	
Ciprofpppppcrpfloxacin-AgNPs	25	26.45 \pm 5.96	2.58 \pm 0.76
	50	51.58 \pm 5.29	
	75	58.52 \pm 10.16	
	100	78.4 \pm 0.45	
Levofloxacin-AgNPs	25	7.64 \pm 1.44	2.55 \pm 0.94
	50	28.84 \pm 2.42	
	75	44.87 \pm 1.65	
	100	72.25 \pm 5.6	
Ascobic acid	25	32.34 \pm 4.04	2.05 \pm 0.03
	50	50.79 \pm 3.48	
	75	65.58 \pm 1.57	
	100	78.96 \pm 0.65	

^aA statistically significant difference in DPPH scavenging activity was found among different nanoparticles of silver at different concentrations with $p < 0.05$ two-way ANOVA.

protecting against oxidative stress.⁶⁵ Both silver nanoparticles derived from *Moringa* and turmeric demonstrate a significant enhancement ($p < 0.05$) in antioxidant activity compared to the extract. *Moringa* is rich in antioxidants, and the conjugation with silver nanoparticles may result in a synergistic effect, enhancing the antioxidant potential. This can be beneficial for combating oxidative stress and related diseases.⁶⁶ Levofloxacin exhibited antioxidant activity at $72.25 \pm 5.6\%$. With an increase in concentration, the activity of scavenging free radicals tends to increase. Cip-AgNPs exhibit a lower value ($78.4 \pm 0.45\%$) compared to that of Lev-AgNPs. The values of these samples are significant for standard ascorbic acid, which shows an activity of $78.96 \pm 0.65\%$.

CONCLUSIONS

This study developed a cost-effective and environmentally friendly method for synthesizing conjugated silver nanoparticles (AgNPs) using antibiotics and plant materials as antibacterial agents, holding great promise as a future direction to address the challenges associated with conventional antibiotic treatments for diseases. In this study, the ciprofloxacin-conjugated AgNPs exhibited a zone of inhibition of 14.4 ± 0.37 mm, which was the highest value observed. On the other hand, the levofloxacin-conjugated AgNPs displayed a zone of inhibition of 13.93 ± 0.2 mm, compared to the antibiotics levofloxacin and ciprofloxacin. Therefore, antibiotic-conjugated silver nanomaterials exhibit higher antibacterial activity compared to that of pure levofloxacin and ciprofloxacin antibiotics. Conjugated silver nanoparticles exhibit a higher surface area compared to larger particles. This increased surface area provides more sites for catalytic reactions to take place, enhancing the overall efficiency. In this investigation, it was determined that nanoparticles of *M. oleifera* and *C. longa* act as strong reducing agents by forming invisible capping coatings around silver, resulting in a zone of inhibition of 13.53 ± 0.32 and 13.73 ± 0.46 , respectively. The FTIR analysis

showed that the carboxyl group of the extracts has a strong interaction with the nanomaterials, thereby stabilizing the surface of the nanoparticles, which is endorsed by previous studies as well.^{67–69}

Additionally, nanomaterials synthesized using this method exhibit excellent antioxidant activity. For instance, the antioxidant activity values are 80.3 ± 3.14 for *Moringa*, 75.22 ± 2.8 for *Curcuma*, 78.4 ± 0.45 for ciprofloxacin-AgNPs, and 72.25 ± 5.6 for levofloxacin-AgNPs. Furthermore, the synthesized AgNPs showed efficient antioxidant efficacy ($>70\%$, $100 \mu\text{g/mL}$) against DPPH, demonstrating that their use would be an encouraging candidate for many biomedical applications. Our work recommends reducing the use of antibiotics by replacing them with nanoconjugates of silver and biologically synthesizing silver nanoparticles. However, there is a further need to analyze the safety of using antibiotic-conjugated silver nanoparticles on animal models.

AUTHOR INFORMATION

Corresponding Author

Andleeb Batool – Department of Zoology, Dr. Nazir Ahmad Institute of Biological Sciences, Government College University, Lahore, 54000 Lahore, Pakistan; orcid.org/0000-0002-1326-8458; Email: andleeb.batool@gcu.edu.pk

Authors

Mehwish Mohy U Din – Department of Zoology, Dr. Nazir Ahmad Institute of Biological Sciences, Government College University, Lahore, 54000 Lahore, Pakistan

Raja Shahid Ashraf – Department of Chemistry, Institute of Chemical Sciences, Government College University, Lahore, 54000 Lahore, Pakistan

Atif Yaqub – Department of Zoology, Dr. Nazir Ahmad Institute of Biological Sciences, Government College University, Lahore, 54000 Lahore, Pakistan

Aneeba Rashid – Department of Botany, Dr. Nazir Ahmad Institute of Biological Sciences, Government College University, Lahore, 54000 Lahore, Pakistan
Nazish Mohy U Din – Sustainable Development Study Center, Government College University, Lahore, 54000 Lahore, Pakistan

Complete contact information is available at:
<https://pubs.acs.org/10.1021/acsomega.3c08927>

Notes

The authors declare no competing financial interest.

ACKNOWLEDGMENTS

The authors acknowledge the assistance provided by the Department of Zoology, Government College University, Lahore.

REFERENCES

- (1) Mansoori, G. A.; Soelaiman, T. F. *Nanotechnology – An Introduction for the Standards Community*; ASTM International, 2005.
- (2) Das, S. K.; Rajabalaya, R.; David, S. R. N. Nanotechnology in Cosmetics: Safety Evaluation and Assessment. In *Nanotechnology*; Taylor & Francis Group, 2019; Vol. 419, p 28.
- (3) Basu, S.; Maji, P.; Ganguly, J. Rapid green synthesis of silver nanoparticles by aqueous extract of seeds of *Nyctanthes arbor-tristis*. *Appl. Nanosci.* **2016**, *6*, 1–5.
- (4) Vanaja, M.; Annadurai, G. *Coleus aromaticus* leaf extract mediated synthesis of silver nanoparticles and its bactericidal activity. *Appl. Nanosci.* **2013**, *3*, 217–223.
- (5) Dikshit, P. K.; Kumar, J.; Das, A. K.; Sadhu, S.; Sharma, S.; Singh, S.; Gupta, P. K.; Kim, B. S. Green synthesis of metallic nanoparticles: Applications and limitations. *Catalysts* **2021**, *11* (8), 902.
- (6) Calderón-Jiménez, B.; Johnson, M. E.; Montoro Bustos, A. R.; Murphy, K. E.; Winchester, M. R.; Vega Baudrit, J. R. Silver nanoparticles: Technological advances, societal impacts, and metrological challenges. *Front. Chem.* **2017**, *5*, 6.
- (7) Hebbalalu, D.; Lalley, J.; Nadagouda, M. N.; Varma, R. S. Greener techniques for the synthesis of silver nanoparticles using plant extracts, enzymes, bacteria, biodegradable polymers, and microwaves. *ACS Sustainable Chem. Eng.* **2013**, *1* (7), 703–712.
- (8) Davies, D. S.; Grant, J.; Catchpole, M. *The Drugs Don't Work: A Global Threat*; Penguin: U.K., 2013.
- (9) Collins, F. S.; Varmus, H. A new initiative on precision medicine. *N. Engl. J. Med.* **2015**, *372* (9), 793–795.
- (10) Hayden, S. C.; Zhao, G.; Saha, K.; Phillips, R. L.; Li, X.; Miranda, O. R.; Rotello, V. M.; El-Sayed, M. A.; Schmidt-Krey, I.; Bunz, U. H. Aggregation and interaction of cationic nanoparticles on bacterial surfaces. *J. Am. Chem. Soc.* **2012**, *134* (16), 6920–6923.
- (11) Wilczewska, A. Z.; Niemirowicz, K.; Markiewicz, K. H.; Car, H. Nanoparticles as drug delivery systems. *Pharmacol. Rep.* **2012**, *64*, 1020–1037.
- (12) Sharma, R. K.; Patel, S.; Pargaien, K. C. Synthesis, characterization and properties of Mn-doped ZnO nanocrystals. *Adv. Nat. Sci. Nanosci. Nanotechnol.* **2012**, *3*, No. 035005.
- (13) Slavin, Y. N.; Asnis, J.; Häfeli, U. O.; Bach, H. Metal nanoparticles: Understanding the mechanisms behind antibacterial activity. *J. Nanobiotechnol.* **2017**, *15*, 65.
- (14) Krishnaraj, C.; Jagan, E. G.; Rajasekar, S.; Selvakumar, P.; Kalaichelvan, P. T.; Mohan, N. J. C. S. B. Synthesis of silver nanoparticles using *Acalypha indica* leaf extracts and its antibacterial activity against water borne pathogens. *Colloids Surf., B* **2010**, *76* (1), 50–56.
- (15) Mao, C.; Xiang, Y.; Liu, X.; Cui, Z.; Yang, X.; Yeung, K. W.; Pan, H.; Wang, X.; Chu, P. K.; Wu, S. Photo-inspired antibacterial activity and wound healing acceleration by hydrogel embedded with Ag/Ag@ AgCl/ZnO nanostructures. *ACS Nano* **2017**, *11* (9), 9010–9021.
- (16) Akhtar, M. S.; Panwar, J.; Yun, Y. S. Biogenic synthesis of metallic nanoparticles by plant extracts. *ACS Sustainable Chem. Eng.* **2013**, *1* (6), 591–602.
- (17) Ahmed, D.; Shah, M. R.; Perveen, S.; Ahmed, S. Cephadrine Coated Silver Nanoparticle their Drug Release Mechanism, and Antimicrobial Potential against Gram-Positive and Gram-Negative Bacterial Strains through AFM. *J. Chem. Soc. Pak.* **2018**, *40* (2), No. e1.
- (18) Matzov, D.; Bashan, A.; Yonath, A. A bright future for antibiotics? *Annu. Rev. Biochem.* **2017**, *86*, 567–583.
- (19) Madela, M. Impact of silver nanoparticles on wastewater treatment in the SBR. *Écol. Environ. Eng.* **2019**, *86*, 00027.
- (20) Que, Z. G.; Torres, J. G. T.; Vidal, H. P.; Rocha, M. A. L.; Pérez, J. C. A.; López, I. C.; Romero, D. D. C.; Reyna, A. E. E. L. M.; Sosa, J. G. P.; Pavón, A. A. S.; Hernández, J. F. Silvernanoparticles – Fabrication, Characterization and Applications. In *Application of Silver Nanoparticles for Water Treatment*; IntechOpen, 2018.
- (21) Yu, Y.; Zhou, Z.; Huang, G.; Cheng, H.; Han, L.; Zhao, S.; Chen, Y.; Meng, F. Purifying water with silver nanoparticles (AgNPs)-incorporated membranes: Recent advancements and critical challenges. *Water Res.* **2022**, *222*, No. 118901.
- (22) Palani, G.; Trilaksana, H.; Sujatha, R. M.; Kannan, K.; Rajendran, S.; Korniejenko, K.; Nykiel, M.; Uthayakumar, M. Silver Nanoparticles for Waste Water Management. *Molecules* **2023**, *28*, 3520.
- (23) Fiorati, A.; Bellingeri, A.; Punta, C.; Corsi, C.; Venditti, I. Silver Nanoparticles for Water Pollution Monitoring and Treatments: Eco-safety Challenge and Cellulose-Based Hybrids Solution. *Polymers* **2020**, *12*, 1635.
- (24) Gao, W.; Thamphiwatana, S.; Angsantikul, P.; Zhang, L. Nanoparticle approaches against bacterial infections. *Wiley Interdiscip. Rev.: Nanomed. Nanobiotechnol.* **2014**, *6* (6), 532–547.
- (25) Jyoti, K.; Baunthiyal, M.; Singh, A. Characterization of silver nanoparticles synthesized using *Urtica dioica* Linn. leaves and their synergistic effects with antibiotics. *J. Radiat. Res. Appl. Sci.* **2016**, *9* (3), 217–227.
- (26) Dar, M. A.; Ingle, A.; Rai, M. Enhanced antimicrobial activity of silver nanoparticles synthesized by *Cryphonectria* sp. evaluated singly and in combination with antibiotics. *Nanomed.: Nanotechnol., Biol. Med.* **2013**, *9* (1), 105–110.
- (27) Fayaz, A. M.; Balaji, K.; Girilal, M.; Yadav, R.; Kalaichelvan, P. T.; Venketesan, R. Biogenic synthesis of silver nanoparticles and their synergistic effect with antibiotics: a study against gram-positive and gram-negative bacteria. *Nanomed.: Nanotechnol., Biol. Med.* **2010**, *6* (1), 103–109.
- (28) Yi, S.; Xia, L.; Lenaghan, S. C.; Sun, L.; Huang, Y.; Burris, J. N.; Zhang, M. Bio-synthesis of gold nanoparticles using English ivy (*Hedera Helix*). *J. Nanosci. Nanotechnol.* **2013**, *13* (3), 1649–1659, DOI: 10.1166/jnn.2013.7183.
- (29) Baharara, J.; Namvar, F.; Ramezani, T.; Mousavi, M.; Mohamad, R. Silver nanoparticles biosynthesized using *Achillea biebersteinii* flower extract: apoptosis induction in MCF-7 cells via caspase activation and regulation of Bax and Bcl-2 gene expression. *Molecules* **2015**, *20* (2), 2693–2706.
- (30) Velgoso, O.; Cizmarova, E.; Malek, J.; Kavuličova, J. Effect of storage conditions on long-term stability of Ag nanoparticles formed via green synthesis. *Int. J. Miner. Metall. Mater.* **2017**, *24*, 1177–1182.
- (31) Vasantharaj, S.; Sathiyavimal, S.; Saravanan, M.; Senthilkumar, P.; Gnanasekaran, K.; Shanmugavel, M.; Shammugavel, M.; Manikandan, E.; Pugazhendhi, A. Synthesis of ecofriendly copper oxide nanoparticles for fabrication over textile fabrics: characterization of antibacterial activity and dye degradation potential. *J. Photochem. Photobiol. B* **2019**, *191*, 143–149.
- (32) Gole, A.; Dash, C.; Ramakrishnan, V.; Sainkar, S. R.; Mandale, A. B.; Rao, M.; Sastry, M. Pepsin– gold colloid conjugates: preparation, characterization, and enzymatic activity. *Langmuir* **2001**, *17* (5), 1674–1679.

- (33) Alsammarraie, F. K.; Wang, W.; Zhou, P.; Mustapha, A.; Lin, M. Green synthesis of silver nanoparticles using turmeric extracts and investigation of their antibacterial activities. *Colloids Surf., B* **2018**, *171*, 398–405.
- (34) Zarei, M.; Jamnejad, A.; Khajehali, E. Antibacterial effect of silver nanoparticles against four foodborne pathogens. *Jundishapur J. Microbiol.* **2014**, *7* (1), No. e8720, DOI: 10.5812/jjm.8720.
- (35) Swapna, G.; Pravalika, B.; Poojitha, J. A Review on Drug-drug interaction studies on Amiodarone and Levofloxacin. *Res. J. Pharmacol. Pharmacodyn.* **2019**, *11* (4), 147–152.
- (36) Maizura, M.; Aminah, A.; Wan Aida, W. M. Total phenolic content and antioxidant activity of kesum (*Polygonum minus*), ginger (*Zingiber officinale*) and turmeric (*Curcuma longa*) extract. *Int. Food Res. J.* **2011**, *18* (2), No. e1.
- (37) Ditta, S. A.; Yaqub, A.; Ullah, R.; Tanvir, F. Evaluation of amino acids capped silver nanoconjugates for the altered oxidative stress and antioxidant potential in albino mice. *J. Mater. Res.* **2021**, *36*, 4344–4359.
- (38) Bhakya, S.; Muthukrishnan, S.; Sukumaran, M.; Muthukumar, M. Biogenic synthesis of silver nanoparticles and their antioxidant and antibacterial activity. *Appl. Nanosci.* **2016**, *6*, 755–766.
- (39) Sharifi-Rad, M.; Pohl, P.; Epifano, F. A.; Ivarez-Suarez, J. M. Green synthesis of silver nanoparticles using astragalus tribuloides delile root extract: characterization, antioxidant, antibacterial, and anti-inflammatory activities. *Nanomaterials* **2020**, *10* (12), 2383.
- (40) Shamel, K.; Ahmad, M. B.; Shabanzadeh, P.; Al-Mulla, E. A. J.; Zamanian, A.; Abdollahi, Y.; Haroun, R. Z.; et al. Effect of *Curcuma longa* tuber powder extract on size of silver nanoparticles prepared by green method. *Res. Chem. Intermed.* **2014**, *40*, 1313–1325.
- (41) Sathishkumar, M.; Sneha, K.; Yun, Y. S. Immobilization of silver nanoparticles synthesized using *Curcuma longa* tuber powder and extract on cotton cloth for bactericidal activity. *Bioresour. Technol.* **2010**, *101* (20), 7958–7965.
- (42) Krishnaraj, C.; Jagan, E. G.; Rajasekar, S.; Selvakumar, P.; Kalaichelvan, P. T.; Mohan, N. Synthesis of silver nanoparticles using *Acalypha indica* leaf extracts and its antibacterial activity against water borne pathogens. *Colloids Surf., B* **2010**, *76* (1), 50–56.
- (43) Zhang, X. F.; Liu, Z. G.; Shen, W.; Gurunathan, S. Silver nanoparticles: Synthesis, characterization, properties, applications, and therapeutic approaches. *Int. J. Mol. Sci.* **2016**, *17*, 1534.
- (44) Tawfeek, H. M.; Abdellatif, A. A.; Abdel-Aleem, J. A.; Hassan, Y. A.; Fathalla, D. Transfersomal gel nanocarriers for enhancement the permeation of lornoxicam. *J. Drug Delivery Sci. Technol.* **2020**, *56*, No. 101540.
- (45) Sampaio, S.; Viana, J. C. Production of silver nanoparticles by green synthesis using artichoke (*Cynara scolymus* L.) aqueous extract and measurement of their electrical conductivity. *Adv. Nat. Sci.: Nanosci. Nanotechnol.* **2018**, *9*, No. 045002, DOI: 10.1088/2043-6254/aae987.
- (46) Masood, N.; Ahmed, R.; Tariq, M.; Ahmed, Z.; Masoud, M. S.; Ali, I.; Hasan, A.; et al. Silver nanoparticle impregnated chitosan-PEG hydrogel enhances wound healing in diabetes induced rabbits. *Int. J. Pharm.* **2019**, *559*, 23–36.
- (47) Sharon, A.; Obed, G. M.; Priya, S. Green Synthesis of Silver Nanoparticles using Plant Extracts and Their Applications for Water Purification and Anti-Diabetic Properties. *Res. J. Chem. Environ.* **2022**, *26*, 4.
- (48) Mohsen, E.; El-Borady, O. M.; Mohamed, M. B.; Fahim, I. S. Synthesis and characterization of ciprofloxacin loaded silver nanoparticles and investigation of their antibacterial effect. *J. Radiat. Res. Appl. Sci.* **2020**, *13* (1), 416–425.
- (49) Mehwish, H. M.; Rajoka, M. S. R.; Xiong, Y.; Cai, H.; Aadil, R. M.; Mahmood, Q.; He, Z.; Zhu, Q. Green synthesis of a silver nanoparticle using *Moringa oleifera* seed and its applications for antimicrobial and sun-light mediated photocatalytic water detoxification. *J. Environ. Chem. Eng.* **2021**, *9* (4), No. 105290.
- (50) Feng, Q. L.; Wu, J.; Chen, G. Q.; Cui, F. Z.; Kim, T. N.; Kim, J. O. A mechanistic study of the antibacterial effect of silver ions on *Escherichia coli* and *Staphylococcus aureus*. *J. Biomed. Mater. Res.* **2000**, *52* (4), 662–668.
- (51) Goswami, M.; Baruah, D.; Das, A. M. Green synthesis of silver nanoparticles supported on cellulose and their catalytic application in the scavenging of organic dyes. *New J. Chem.* **2018**, *42* (13), 10868–10878.
- (52) Zhao, X.; Yan, L.; Xu, X.; Zhao, H.; Lu, Y.; Wang, Y.; Shi, J.; et al. Synthesis of silver nanoparticles and its contribution to the capability of *Bacillus subtilis* to deal with polluted waters. *Appl. Microbiol. Biotechnol.* **2019**, *103*, 6319–6332.
- (53) Mohammed, G. M.; Hawar, S. N. Green Biosynthesis of Silver Nanoparticles from *Moringa oleifera* Leaves and Its Antimicrobial and Cytotoxicity Activities. *Int. J. Biomater.* **2022**, *2022*, No. 4136641, DOI: 10.1155/2022/4136641.
- (54) Shankar, P. D.; Shobana, S.; Karuppusamy, I.; Pugazhendhi, A.; Ramkumar, V. S.; Arvindnarayan, S.; Kumar, G. A review on the biosynthesis of metallic nanoparticles (gold and silver) using bio-components of microalgae: Formation mechanism and applications. *Enzyme Microb. Technol.* **2016**, *95*, 28–44, DOI: 10.1016/j.enzmictec.2016.10.015.
- (55) Gallón, S. M. N.; Alpaslan, E.; Wang, M.; Larese-Casanova, P.; Londoño, M. E.; Atehortúa, L.; Pavón, J. J.; Webster, T. J. Characterization and study of the antibacterial mechanisms of silver nanoparticles prepared with microalgal exopolysaccharides. *Mater. Sci. Eng. C* **2019**, *99*, 685–695.
- (56) Chougule, S. S.; Gurme, S. T.; Jadhav, J. P.; Dongale, T. D.; Tiwari, A. P. Low density polyethylene films incorporated with Biosynthesized silver nanoparticles using *Moringa oleifera* plant extract for antimicrobial, food packaging, and photocatalytic degradation applications. *J. Plant Biochem. Biotechnol.* **2021**, *30*, 208–214.
- (57) Saadh, M. J. Effect of silver nanoparticles on the antibacterial activity of Levofloxacin against methicillin-resistant *Staphylococcus aureus*. *Eur. Rev. Med. Pharmacol. Sci.* **2021**, *25* (17), 5507–5510.
- (58) Liu, C.; Luo, L.; Liu, L. Antibacterial effect and mechanism of silver-carried zirconium glycine-N, N-dimethylenephosphonate as a synergistic antibacterial agent. *Inorg. Chem. Commun.* **2019**, *107*, No. 107497.
- (59) Chokshi, A.; Sifri, Z.; Cennimo, D.; Horng, H. Global contributors to antibiotic resistance. *J. Global Infect. Dis.* **2019**, *11* (1), 36. Tyagi, P.; Singh, M.; Kumari, H.; Kumari, A.; Mukhopadhyay, K. Bactericidal activity of curcumin I is associated with damaging of bacterial membrane. *PLoS One* **2015**, *10* (3), e0121313.
- (60) Shome, S.; Talukdar, A. D.; Choudhury, M. D.; Bhattacharya, M. K.; Upadhyaya, H. Curcumin as potential therapeutic natural product: a nanobiotechnological perspective. *J. Pharm. Pharmacol.* **2016**, *68* (12), 1481–1500.
- (61) Loo, Y. Y.; Rukayadi, Y.; Nor-Khaizura, M. A. R.; Kuan, C. H.; Chieng, B. W.; Nishibuchi, M.; Radu, S. In vitro antimicrobial activity of green synthesized silver nanoparticles against selected gram-negative foodborne pathogens. *Front. Microbiol.* **2018**, *9*, 1555.
- (62) Yin, I. X.; Zhang, J.; Zhao, I. S.; Mei, M. L.; Li, Q.; Chu, C. H. The Antibacterial Mechanism of Silver Nanoparticles and Its Application in Dentistry. *Int. J. Nanomed.* **2020**, *15*, 2555–2562.
- (63) Shousha, W. G.; Aboulthana, W. M.; Salama, A. H.; Saleh, M. H.; Essawy, E. A. Evaluation of the biological activity of *Moringa oleifera* leaves extract after incorporating silver nanoparticles, in vitro study. *Bull. Natl. Res. Centre* **2019**, *43* (1), 1–13.
- (64) Younes, I.; Sellimi, S.; Rinaudo, M.; Jellouli, K.; Nasri, M. Influence of acetylation degree and molecular weight of homogeneous chitosans on antibacterial and antifungal activities. *Int. J. Food Microbiol.* **2014**, *185*, 57–63.
- (65) Selvan, D. A.; Mahendiran, D.; Kumar, R. S.; Rahiman, A. K. Garlic, green tea and turmeric extracts-mediated green synthesis of silver nanoparticles: Phytochemical, antioxidant and in vitro cytotoxicity studies. *J. Photochem. Photobiol. B* **2018**, *180*, 243–252.
- (66) Öztürk, B. Y.; Gürsu, B. Y.; Dağ, İ. Antibiofilm and antimicrobial activities of green synthesized silver nanoparticles using marine red algae *Gelidium corneum*. *Process Biochem.* **2020**, *89*, 208–219.

(67) Monsef, R.; Salavati-Niasari, M. Electrochemical sensor based on a chitosan-molybdenum vanadate nanocomposite for detection of hydroxychloroquine in biological samples. *J. Colloid Interface Sci.* **2022**, *613*, 1–14.

(68) Mir, N.; Salavati-Niasari, M. Preparation of TiO₂ nanoparticles by using tripodal tetraamine ligands as complexing agent via two-step sol–gel method and their application in dye-sensitized solar cells. *Mater. Re ups. Bull.* **2013**, *48* (4), 1660–1667.

(69) Zinatloo-Ajabshir, S.; Baladi, M.; Salavati-Niasari, M. Enhanced visible-light-driven photocatalytic performance for degradation of organic contaminants using PbWO₄ nanostructure fabricated by a new, simple and green sonochemical approach. *Ultrason. Sonochem.* **2021**, *72*, No. 105420.